Proceedings of the 11th Brazilian Congress of Thermal Sciences and Engineering -- ENCIT 2006
Braz. Soc. of Mechanical Sciences and Engineering -- ABCM, Curitiba, Brazil,- Dec. 5-8, 2006

Paper CIT06-0258

ANALYSIS OF TWO MOLECULAR DIFFUSION MODELS FOR PREDICTING WAX DEPOSITION IN LAMINAR FLOW

Mao Ilich Romero
Departamento de Engenharia Mecânica, PUC-RIO, 22453-900, RJ
mao@mec.puc-rio.br

Angela Ourivio Nieckele
Departamento de Engenharia Mecânica, PUC-RIO, 22453-900, RJ
nieckele@mec.puc-rio.br

Luis Fernando Alzuguir Azevedo
Departamento de Engenharia Mecânica, PUC-RIO, 22453-900, RJ
lfaa@mec.puc-rio.br

Abstract. *Deposition of high molecular weight paraffins on the inner wall of subsea production and transportation pipelines continues to be a critical operational problem faced by the petroleum industry. Molecular diffusion, Brownian diffusion, shear dispersion and gravity settling are some of the possible mechanism responsible for wax deposition cited in the literature. Although, molecular diffusion is employed in the vast majority of the deposition models available in the literature, it is still not clear which one is the most relevant mechanism. In the present study a numerical analysis of the wax deposition is performed employing only the molecular diffusion model. The wax deposition is determined considering oil flowing in the laminar regime, through a rectangular channel. Two mathematical models are investigated. The first formulation is one-dimensional and the wax deposition rate is determined indirectly from the heat flux through the channel wal., The second formulation is two-dimensional and the wax deposition rate is a function of the paraffin concentration gradient. The finite volume method was selected to solve the conservation equations of mass, energy and mass fraction, coupled with a diffusive equation to describe the growth of the wax deposit. A moving mesh was employed to account for the reduction of the flow cross section due to the paraffin deposition. Additionally, the influence of the paraffin latent heat was investigated. The results obtained showed the same trends for both models, but a much slower deposition rate was observed for the first one. The results obtained numerically were compared with experimental results found in the literature for four Reynolds numbers. As expected, the deposited layer is comparatively thinner for the higher flow rates represented by the higher value of the Reynolds number.*

Keywords: *wax deposition, pipeline, laminar flow, molecular diffusion*

1. Introduction

Wax deposition in production and transportation pipelines continues to be a relevant problem for the industry, particularly in offshore operations. The crude oil flows out of the reservoir at, typically, 60 ^{o}C into the production pipelines. These lines carry the oil to the platforms and from the platforms to shore. At large water depths, the ocean temperature at the bottom is of the order of 5 ^{o}C. The solubility of wax in the oil is a decreasing function of temperature. As the oil flows, it loses heat to the surrounding water. If the crude oil temperature falls below the Wax Appearance Temperature (WAT), the wax may precipitate and deposit along the inner walls of the pipeline. The accumulation of the deposited material may lead to increased pumping power, decreased flow rate or even to the total blockage of the line with loss of production and capital investment.

A significant research effort has been devoted to the understanding and modeling of the wax deposition problem (Burger et al., 1981, Brown et al., 1993, Creek et al., 1999 and Svendsen, 1993). This is a complex problem that involves several disciplines such as thermodynamics, heat transfer, mass transfer, crystal growth and fluid dynamics. An accurate prediction of the temporal and spatial distributions of the deposited wax along the pipeline would be invaluable information that would help in the design stages of the field, as well as in the scheduling of interventions in the pipeline, in order to assure the flow of oil at the desired rates.

A detailed critical review of the literature was prepared as part of a research project on wax deposition (Azevedo and Teixeira, 2003). One of the key works analyzed in this review was that of Burger et al. (1981) where the possible mechanisms responsible for wax deposition were identified. These mechanisms are molecular diffusion, Brownian diffusion, shear dispersion, and gravitational settling. Molecular diffusion has been widely accepted as the dominant deposition mechanism, and has been included in the vast majority of the models presented in the open literature (e.g., Ribeiro et al., 1997, Fusi, 2003). An observation of the deposition models available in the literature shows that they all make use of adjusting constants to fit the model predictions to field or laboratory data. In our view this practice, totally justified for yielding good predictions for particular lines, complicates the task of assessing the relative importance of each deposition mechanism. Therefore, in the review article mentioned above, Azevedo and Teixeira (2003) concluded that there was no experimental evidence to confirm that molecular diffusion is the dominant deposition mechanism.

Recently Leiroz et al (2005) presented a comparison between the experimental data of Leiroz (2004) and the predictions of a one-dimensional model for wax deposition, considering only the molecular diffusion mechanism. The experiments where conducted under controlled conditions and allowed, seemingly for the first time, the determination of the spatial and temporal distributions of the deposited wax. The comparison of the results presented a large discrepancy between experiments and numerical predictions for the transient regime. Both the experiments and the simulations were conducted for laminar flow conditions.

The present paper presents results of an ongoing research effort aimed at identifying the relative importance of the deposition mechanisms. To this end, the diffusion-based model of Leiroz et al.(2005) was improved by the implementation of a two-dimensional formulation where the concentration equation for the liquid wax was also solved. Therefore, two mathematical models are compared; the first formulation is one-dimensional and the wax deposition rate is determined by an indirect way from the heat flux through the channel wall, while the second formulation is two-dimensional and the wax deposition rate is calculated based on the paraffin concentration gradient at the deposit.. The mathematical model developed was employed to simulate the same conditions of the laboratory tests conducted by Leiroz(2004). Those were tests conducted under controlled conditions employing simple oil-wax mixtures with known properties., flowing through a test section well-defined boundary and initial conditions. In the simulations, the measured properties of the test fluids were employed. No constants were adjusted to fit the predicted results to the measured data, as it is normally done with models that predict field operations. It is believed that the comparison between the predicted and experimental results for these simple configurations would allow a better assessment of the relative importance of the deposition mechanisms.

2. Mathematical model

The main objective of the present research is to help identify the relative importance of the wax deposition mechanisms proposed in the literature. The idea was to develop a simple model that incorporated one deposition mechanism at a time and compare the predictions obtained with the simple experiments conducted. In the present paper, the molecular diffusion model is investigated, since this is the most widely accepted mechanism. Different approximations are made and two mathematical diffusion models are developed and compared.

The geometry of the problem modeled is presented schematically in Figure (1), where symmetry in relation to the horizontal axis was enforced. The oil and wax solution enters the domain, which has a rectangular cross section (height a and width W), with a uniform temperature T_i and a constant flow rate $\dot{m}$. In all cases studied T_i was always above the wax appearance temperature for the solution, T_{WAT}. The channel length is L. The solution loses energy to the ambient at temperature T_{amb} through the side glass walls with an overall heat transfer coefficient U_{lat}. Cold water with constant temperature T_{H2O} flows through channels connected to the upper and lower copper walls. Due to the high thermal conductivity of the copper, its temperature was assumed to be equal to the water temperature. The working fluid was considered as a binary homogeneous solution of oil, the solvent, and wax, the solute. The wax deposition begins when the oil interface temperature T_{int} is lower than the wax appearance temperature T_{WAT}. The wax deposition thickness is δ.

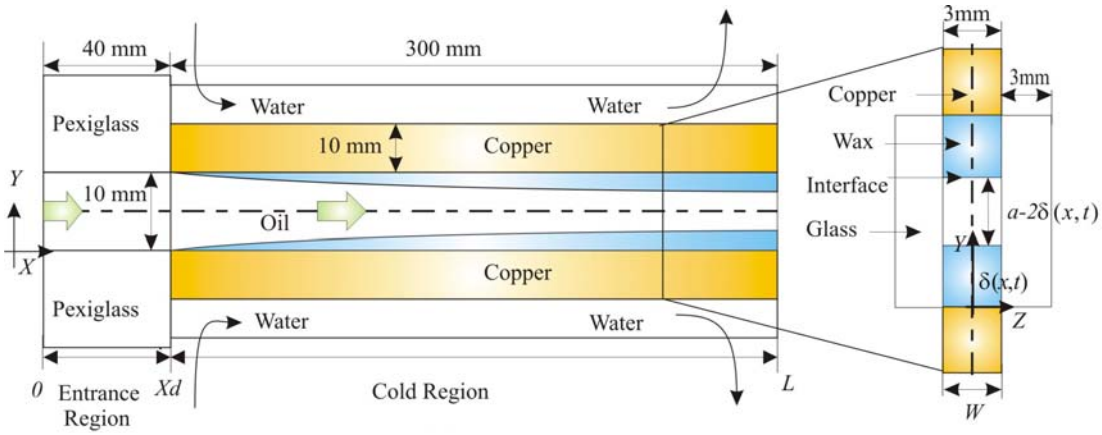

(a) full domain (b) side view

Figure 1. Schematic view of the computational domain

At the beginning of the process, the water flows at the same temperature as the inlet oil. So, at time equal to zero, the whole apparatus is nearly at the same temperature equal to the mixture inlet temperature, since the heat losses to the ambient through the glass walls area quite small. Thus, at t= 0, the interface temperature T_{int} is larger than T_{WAT}, therefore both δ and $d\delta/dt$ are zero. The growth of the deposited layer was accounted for by a molecular diffusion mechanism, as suggested by Burger et al. (1981). In this model, the deposition occurs when $T_{int} < T_{WAT}$ and the diffusion flux of wax toward the cold wall is estimated by Fick's law of diffusion,

$$\frac{\partial m_{wax}}{\partial t} = -\rho\, \mathcal{D}_{wax}\, W\, dx \left.\frac{\partial \omega}{\partial y}\right|_{int} \quad ; \quad m_{wax} = \rho_{wax}(1-\phi)\, W\, \delta\, dx \tag{1}$$

where ρ. is the mixture density, $\mathcal{D}_{wax}$ is the molecular diffusion coefficient of the liquid wax in the solvent oil, ω is the concentration (or volume fraction of wax in the solution), m_{wax} is the wax mass deposited in the length dx, ρ_{wax} is the solid wax density and ϕ is the porosity of the oil-filled wax deposit, and it is given by the ratio of the liquid mass inside the deposit by the total mass of the deposit. $m=\rho\, W\, (a/2 - \delta)\, dx$ is the fluid mass contained in an elementary volume. Rearranging Eq. (1), the wax deposition can be obtained from

$$\frac{\partial \delta}{\partial t} = -\frac{\rho}{\rho_{wax}} \frac{\mathcal{D}_{wax}}{(1-\phi)} \left.\frac{\partial \omega}{\partial y}\right|_{int} \tag{2}$$

The difference between the diffusion models studied is related with the determination of the concentration gradient at the interface of the deposit. The first model is one-dimensional, while the second is two-dimensional. The two models are described in the following sections.

2.1. One-dimensional model

The first model is one dimensional, and the schematic view of the computational domain seen in Fig. (2) can help its description. In this model, the concentration gradient of ω (or volume fraction of wax in the solution) at the interface, in Eq. (2) was approximated by the product of the wax solubility coefficient $\partial\omega/\partial T$ by the interface temperature gradient. Thus,

$$\left.\frac{\partial \omega}{\partial y}\right|_{int} = \left.\frac{\partial \omega}{\partial T}\frac{\partial T}{\partial y}\right|_{int} \tag{3}$$

Since the model is one-dimensional, the temperature gradient could not be directly determined. Thus, it was obtained from the heat flux through the interface q_{int}, which was determined from the heat transfer coefficient at the interface h_i, and the temperature difference between the oil mixture T and the interface T_{int}, as

$$-k_m \left.\frac{\partial T}{\partial y}\right|_{int} = q_{int} = h_i\,(T - T_{int})\,. \tag{4}$$

where k_m is the oil mixture thermal conductivity. Substituting Eq. (4) into Eqs (3) and (2), the wax deposition can be obtained from

$$\frac{d\,\delta}{d\,t} = \frac{\rho}{\rho_{wax}} \frac{\mathcal{D}_{wax}}{(1-\phi)} \frac{\partial \omega}{\partial T} \frac{h_i}{k_m} (T - T_{int}) \tag{5}$$

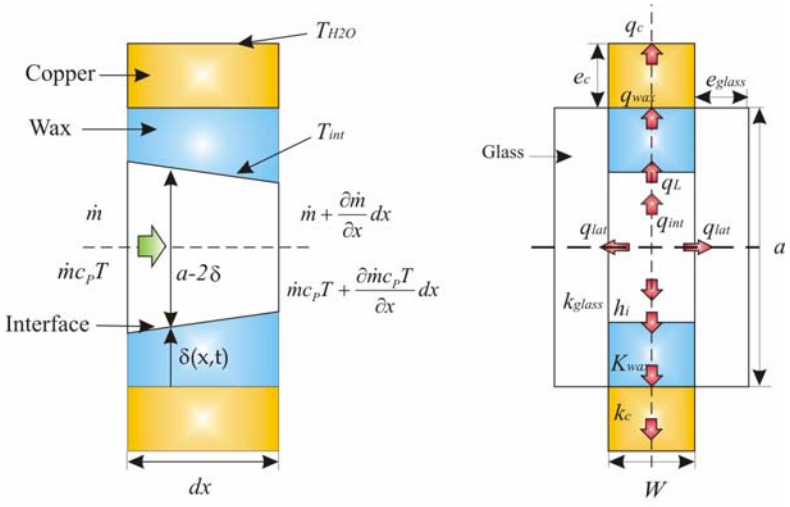

(a) front view (b) side view

Figure 2. Schematic view of the computational domain for the one-dimensional model.

The heat transfer coefficient was determined from the local Nusselt number Nu_i correlation for the developing thermal entry region for parallel-plate channels, with constant temperature boundary condition, as given by Incropera, DeWitt, (1990). The Nusselt number Nu_i is a function of the dimensionless coordinate along the channel *X,* defined as

$$Nu_i = \frac{h_i\, D_h}{k_m} \quad ; \quad X = \frac{x / D_h}{\mathbf{Re}_x\, \mathbf{Pr}} \quad ; \quad D_h = \frac{4A_t}{2\,(W + a - 2\delta)} \quad ; \quad \mathbf{Re}_x = \frac{\dot{m}\, D_h}{A_t\, \mu} \quad ; \quad \mathbf{Pr} = \frac{\mu\, c_p}{k_m} \tag{6}$$

where D_h is the hydraulic diameter, $A_t = 2\ W\ (\ a\ -\ 2\ \delta\ )$ is the cross section area, which decreases as the wax is deposited, $\dot{m}$ is the mass flow rate of the oil mixture, μ is the oil dynamic viscosity and c_p the specific heat at constant pressure.

To determine the axial variation of the bulk fluid temperature *T, t*he energy equation was solved. The energy equation for the solution applied to the control volume of Figure (2), neglecting axial diffusion, is

$$\frac{\partial\,(m'\, cp\, T)}{\partial\, t} + \frac{\partial\,(\dot{m}\, cp\, T)}{\partial\, x} + q_{int}\ 2\,W + q_{lat}\, 2(a - 2\delta) = 0 \tag{7}$$

where $m' = \rho\ A_t$ is the mass of solution per unit length. Heat losses through the transverse channel direction were computed taking into account the convective thermal resistance within the channel and the deposited layer q_{int}. Heat losses through the glass lateral walls were also considered. q_{lat}.

$$q_{lat} = U_{lat}\,(T - T_{amb}) \quad ; \quad \frac{1}{U_{lat}} = \frac{1}{h_i} + \frac{e_{glass}}{k_{glass}} \tag{8}$$

where T_{amb} is the ambient temperature, and U_{lat} is the overall side wall heat transfer coefficient, which is formed by the solution forced convection resistance at the inner wall h_i, the conduction resistance of the glass with thickness e_{glass} and thermal conductivity k_{glass}.

The interface temperature T_{int} was determined by an energy balance at the wax/solution interface, where the latent heat of the wax was taken into consideration at the wax/solution interface, i.e., the difference in heat fluxes from each side of the interface is proportional to the wax latent heat λ and rate of mass deposited, as

$$(q_{int} - q_{wax})\, W\, dx = \frac{d\, m_{wax}}{dt}\, \lambda \tag{9}$$

where q_{wax} is the heat flux through the solid wax and copper wall, and it is determined by assuming that the outer cooper wall has the same temperature as the flowing cooling water T_{H2O}

$$q_{wax} = U_{wax}\,(T_{int} - T_{H2O}) \quad ; \frac{1}{U_{wax}} = \frac{\delta}{k_{wax}} + \frac{e_c}{k_c} \tag{10}$$

U_{wax} is the overall heat transfer coefficient at the wax side, formed by the conduction resistance of the copper walls and the wax deposit, that have, respectively, thicknesses e_c and δ, and thermal conductivities k_c and k_{wax}. The interface temperature can then be determined by

$$T_{int} = \frac{h_i T + U_{wax} T_{H2O} - \rho_{wax}\ \lambda\ (d\delta / d\,t)}{h_i + U_{wax}} \tag{11}$$

Hot solution is introduced in the channel with a temperature higher that the T_{WAT} for the mixture. The initial condition for the problem was a steady state flow, with the solution exchanging heat with water flowing at the same inlet hot temperature. The experiment started by a step change reduction in the water temperature to a value below T_{WAT}.

The energy equation was discretized based on the finite volume method (Patankar, 1980), with the upwind scheme to treat the convection term. A totally implicit procedure was employed to handle the time integration of both Eq. (5) and (7). The set of algebraic equations was solved by the TDMA algorithm.

2.2. Two-dimensional model

In order to determine the wax deposition rate for the second model, Eq. (2) was applied directly. The wax concentration gradient at the interface was obtained by the solution of the wax volume fraction conservation equation, which was applied to an infinitesimal control volume $d\,\forall$, with surface *SC* as illustrated in Figure 3,

$$\frac{\partial}{\partial t}\int_{d\forall}\rho\,\omega\,d\forall+\int_{SC}\rho\,\omega\,\vec{u}\bullet\vec{n}\,dA=\int_{SC}\overrightarrow{m''}\bullet\vec{n}\,dA \tag{12}$$

where t is time, $\vec{u}$ is the velocity vector, $\overrightarrow{m''}=-\rho\,\mathcal{D}_{wax}\,\mathbf{grad}\,\omega$ is the mass diffusive flux and $\vec{n}$ is the unit vector normal to the surface SC.

Since the wax deposition, given by Eq. (2), can only occur when the interface temperature is below T_{WAT}, the temperature distribution is a necessary information, which is obtained from the solution of the energy equation applied to the same control volume $d\forall$,

$$\frac{\partial}{\partial t}\int_{d\forall}\rho\,c_p\,T\,d\forall+\int_{SC}\rho\,c_p\,T\,\vec{u}\bullet\vec{n}\,dA=\int_{SC}\overrightarrow{q''}\bullet\vec{n}\,dA \tag{13}$$

where $\overrightarrow{q''}=-k_m\,\mathbf{grad}\,T$ is the diffusive heat flux. Heat losses through the transverse channel direction were computed taking into account the convective thermal resistance within the channel and the conductive resistance in the deposited layer and in the channel metallic walls. Heat losses through the glass lateral walls were also considered.

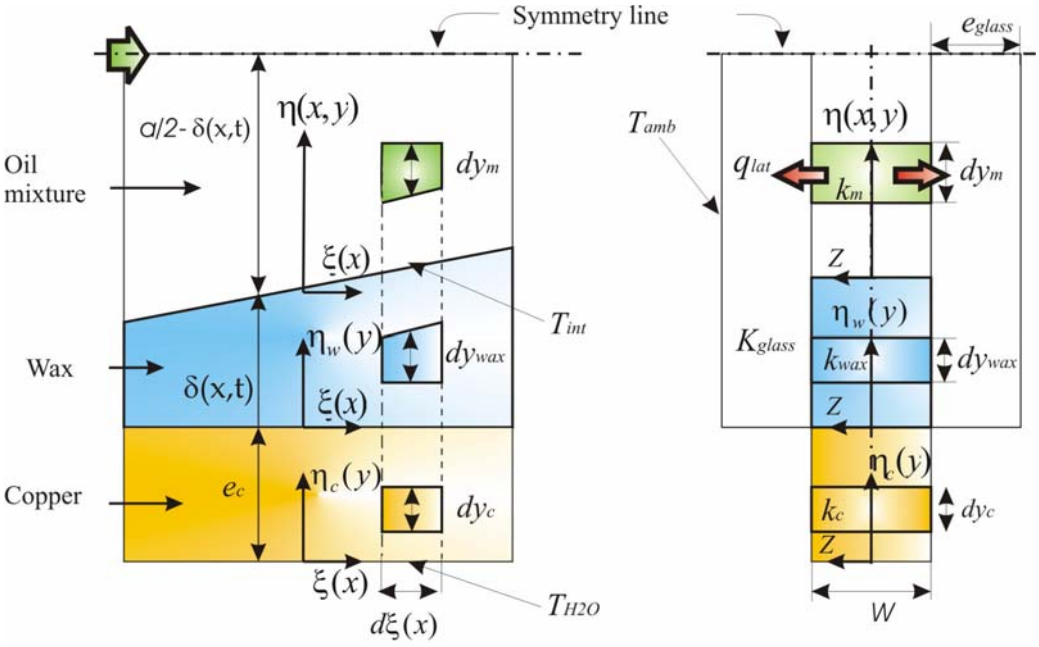

(a) front view (b) side view

Figure 3. Schematic view of the computational domain for the two-dimensional model

To simplify the problem, the flow field was considered as locally hidrodynamically fully developed, i.e., a parabolic velocity profile in the vertical direction was prescribed, with the mean axial velocity varying with the axial coordinate due to the decrease in channel cross sectional area caused by the wax accumulation. The velocity field was prescribed as

$$\vec{u}=u\,\vec{i}\qquad;\qquad u=1.5\,u_m\left[1-y^2/(a/2-\delta)^2\right]\qquad;\qquad u_m=\frac{\dot{m}}{\rho\,(a-2\,\delta)\,W}. \tag{14}$$

Since during the wax deposition process, the flow cross section area varies; it is convenient to apply the conservation equations, Eqs. (12) and (13), to a moving curvilinear coordinate system as illustrated in Fig. (4), where the following dimensionless coordinate system was introduced

$$\xi=x\;;\qquad \eta=\frac{y-\delta}{a/2-\delta}\qquad;\qquad \tau=t \tag{15}$$

Considering constant properties, the wax volume fraction and energy conservation equations, eqs. (12) and (13), can be written as (Romero, 2005)

$$\frac{\partial (Ja\,\omega)}{\partial \tau} + \frac{\partial \left(Ja\ \tilde{U}\ \omega\right)}{\partial \xi} + \frac{\partial \left(h_\xi\ \tilde{V}\ \omega\right)}{\partial \eta} = \mathcal{D}_{wax} \frac{\partial}{\partial \xi}\left(Ja \frac{\partial\ \omega}{\partial \xi} + \beta \frac{\partial\ \omega}{\partial \eta}\right) + \mathcal{D}_{wax} \frac{\partial}{\partial \eta}\left(\frac{h_\xi^2}{Ja} \frac{\partial\ \omega}{\partial \eta} + \beta \frac{\partial\ \omega}{\partial \xi}\right) \tag{16}$$

$$\frac{\partial (JaT)}{\partial \tau} + \frac{\partial \left(Ja\ \tilde{U}\ T\right)}{\partial \xi} + \frac{\partial \left(h_\xi\ \tilde{V}\ T\right)}{\partial \eta} = \alpha \frac{\partial}{\partial \xi}\left(Ja \frac{\partial\ T}{\partial \xi} + \beta \frac{\partial\ T}{\partial \eta}\right) + \alpha \frac{\partial}{\partial \eta}\left(\frac{h_\xi^2}{Ja} \frac{\partial\ T}{\partial \eta} + \beta \frac{\partial\ T}{\partial \xi}\right) + \frac{U_{lat}\ (T - T_\infty)\ Ja}{\rho\, c_p} \tag{17}$$

where $\mathcal{D}_{wax}$ is the wax molecular diffusion coefficient and $\alpha = k/(\rho\, c_p)$ is the mixture thermal diffusivity. Ja is the Jacobian of the coordinate transformation matrix, h_ξ is a metric in the ξ direction and β is a geometric parameter associated with the non-orthogonallity of the coordinate system. $\tilde{U}$ and $\tilde{V}$ are the contra-variant relative velocity components in the ξ and η directions, respectively. These variables are defined as

$$Ja = a/2 - \delta \quad ; \quad h_\xi = [1 + \beta^2]^{1/2} \quad ; \quad \beta = (\eta - 1)\frac{\partial \delta}{\partial x} \tag{18}$$

$$\tilde{U} = u \quad ; \quad \tilde{V} = \frac{(\eta - 1)}{h_\xi} \frac{\partial \delta}{\partial t} - \frac{\beta}{h_\xi} u \tag{19}$$

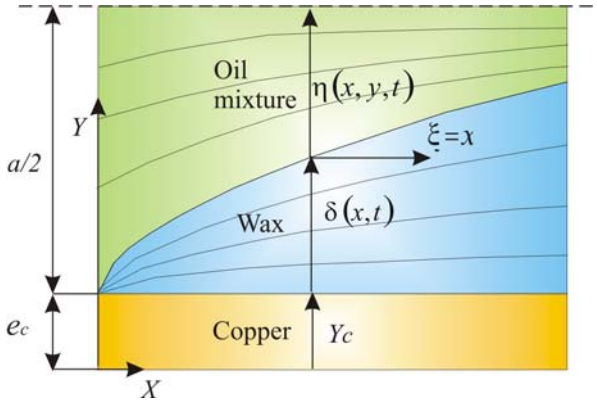

Figure 4. Coordinate system.

At the beginning of the process, the interface temperature is equal to the cold water temperature T_{H2O}, and the wax deposit is zero. However, as the wax deposit increases, the conduction equation at the wax region is also solved.

To solve the set of Eqs. (16) and (17), the following boundary conditions were considered: uniform temperature and wax concentration at the inlet and negligible diffusion at the outlet. At the upper boundary a symmetry condition was defined. The wax concentration at the interface is determined at the interface temperature from the equilibrium wax solubility curve determined experimentally by Leiroz, 2004. The critical boundary condition is at the interface between the fluid and wax deposit, since it controls the process. At this boundary, a heat balance is defined, taking into account the wax latent heat λ, as given by Eq. (9), and the heat flux is determined at both sides of the interface based on the temperature gradient at each side (the subscript *sol* refers to the mixture side and *wax* to the solid wax side).

$$(q_{int} - q_{wax})\, W\, dx = \frac{d\ m_{wax}}{dt}\, \lambda \quad \text{where} \quad q_{int} = -k_m \left.\frac{\partial T}{\partial y}\right|_{sol} \quad ; \quad q_{wax} = -k_{wax} \left.\frac{\partial T}{\partial y}\right|_{wax} \tag{20}$$

The energy equation was discretized based on the finite volume method (Patankar, 1980), with the upwind scheme to treat the convection term. A totally implicit procedure was employed to handle the time integration of both Eq. (16) and (17). The set of algebraic equations was solved by the TDMA line by line algorithm.

Mesh and time step independence tests were performed, until the solutions for different meshes and time steps agreed to within 0.1%. The results presented in the present paper were obtained with 50 control volumes along the axial direction and with 151 control volumes at the η direction for the fluid region and 21 in the wax region and 21 in the copper. The time step was set as 3 s.

3. Results and Discussion

The conservation equations presented for the one-dimensional and two-dimensional models were solved and compared with the experimental data of Leiroz, 2004. To allow a fair comparison, the same geometry used in the

experiments was modeled and the same fluid and wax properties from the work of Leiroz, 2004 were used. The following properties for the solution and solid wax were considered to be equal, being set as: density ρ = 844 kg/m^3, specific heat c_p=2017 J/(kg K), thermal conductivity, k = 0.23 W/(m K). The molecular diffusion coefficient was taken as $\mathcal{D}_{wax} = 2.09 \times 10^{-10}$ m^2/s, the wax latent heat as λ=2.64 × 10^5 J/kg, and the solution absolute viscosity as $\mu = 1.02 \times 10^{-2}$ Pa s. The wax deposit porosity was assumed to de equal to $\phi = 0.86$ based on information from Burger et al., 1981. The fluid inlet and wall temperatures were 40 and 15^{o}C respectively. The T_{WAT} for the test solution was equal to 36^{o}C.

The equilibrium wax solubility curve determined experimentally by Leiroz (2004) was given by

$$\omega = 1.021 \times 10^{-9} \; T^{5.13} \qquad \text{with } T \text{ in } {}^{o}\text{C}. \tag{21}$$

Solutions were obtained for four different values of the Reynolds number **Re,** namely**,** 366, 516, 688, 858. The definition employed for **Re** is

$$\mathbf{Re} = \frac{\dot{m}\, D_h}{\mu\, W\, a} \qquad ; \qquad D_h = \frac{2\, W\, a}{(W + a)} \tag{22}$$

Figures (5) through (9) show results for the thickness of the deposited layer given in millimeters as a function of the axial coordinate of the channel, given also in millimeters. Figure (5) presents the wax deposit growth for **Re**=858. Each curve represents a different time counted from the initiation of the cooling of the walls. The symbols correspond to the experimental data of Leiroz(2004), the solid lines correspond to the numerical solution obtained with the two-dimensional model, while the dashed lines correspond to the one-dimensional model prediction. Figures (6) through (9) present a comparison of the steady state results obtained with both models with the experimental data of Leiroz (2004), for the four Reynolds numbers investigated.

Analysing Fig. (5), it can be seen that after four hours, no more deposit growth was verified, indicating the attainment of a steady condition. An observation of the experimental data of Fig. (5) reveals the rapid growth of the deposit layer. Indeed, the first 10 minutes of deposit accumulation are responsible for nearly 50% of the final, steady state thickness. The numerical prediction for the steady state deposition profile is quite good over the whole length of the channel with the two-dimensional model, while, for this Reynolds number, the one-dimensional model over-predicted the deposited layer, for the steady state regime. In spite of the reasonable steady state results, both models were unable to predict the transient behavior of the deposit. In fact, the diffusion-based model was not able to even predict the correct trend for the spatial distribution of the deposited layer. While the experiments display a monotonic increase of the deposited layer for all time instants, the models predict an increase in the deposit at the channel entrance followed by a decrease, which is the opposite trend in relation to the experiments. It should be mentioned that all models available in the literature display similar up-and-down behavior as the present model (eg. Brown et al, 1993 and Ribeiro et al, 1997). The transient 1-D model prediction is even worse than the 2-D model prediction, leading to much larger time to attain the steady state regime. These results indicate that the 1-D model predicts a smaller temperature gradient than the 2-D model.

The reasonable agreement with experiments obtained for the steady state regime can be explained by the fact that the deposit can only occur while the interface temperature is lower than T_{WAT}, and this value is controlled by the conduction heat flux through the wax layer. As the deposit layer increases, for the same heat flux from the cold water, the interface temperature increases, until it reaches T_{WAT}, when no more deposition occurs. Considering this argument, the final steady state deposit profile should be governed by the steady state position of the isotherm corresponding to T_{WAT}, which is a heat-transfer-governed problem with no influence of the mass transfer process.

Figures (6) through (9) present a comparison of both numerical models and experimental results obtained for the four Reynolds numbers investigated, at the steady state condition. As expected, the deposited layer is comparatively thinner for the higher flow rates represented by the higher value of the Reynolds number. For the steady state regime, it can be observed that a reasonable quantitative agreement and same trends are obtained. It can be seen that the 2-D model presents a better agreement near the entrance of the channel in relation to the 1-D model, which substantially over-predicted the amount of deposit at that region. It can also be seen, that the quality of the agreement is reduced as the Reynolds number decreases with the 2-D model and the opposite trend is observed with the 1-D model. An observation of the results shows that the 1-D model always predicts larger deposits at steady state. It should be pointed out that the 1-D model strongly depends on the internal Nusselt number correlation to determine the heat flux at the interface, while for the 2-D model; the heat flux is obtained from the temperature profile calculated, without any empirical correlation.

This poor level of agreement presented here is encountered in all models available in the literature. They all use molecular diffusion as the deposition mechanism. What is normally done in the literature is to adjust the numerical predictions to the experimental data via the modification of the constant that incorporates the molecular diffusion coefficient, porosity, and other parameters. This procedure, in our view, is responsible for the popularity of the molecular-diffusion based models. Here, for the first time, we show that when actual properties are used, the molecular diffusion based mechanism as normally implemented in the literature is not capable of predicting the transient behavior of the deposition thickness even for this very simple configuration studied.

The reason for the discrepancy between measured and predicted results is no yet known. It is conceivable that deposition mechanisms other than molecular diffusion might be relevant. It is also plausible that a more elaborate model that solves the fully three dimensional momentum and energy equations coupled with conservation equations for the chemical species might yield better agreement with the experimental data. This line of research is presently being conducted.

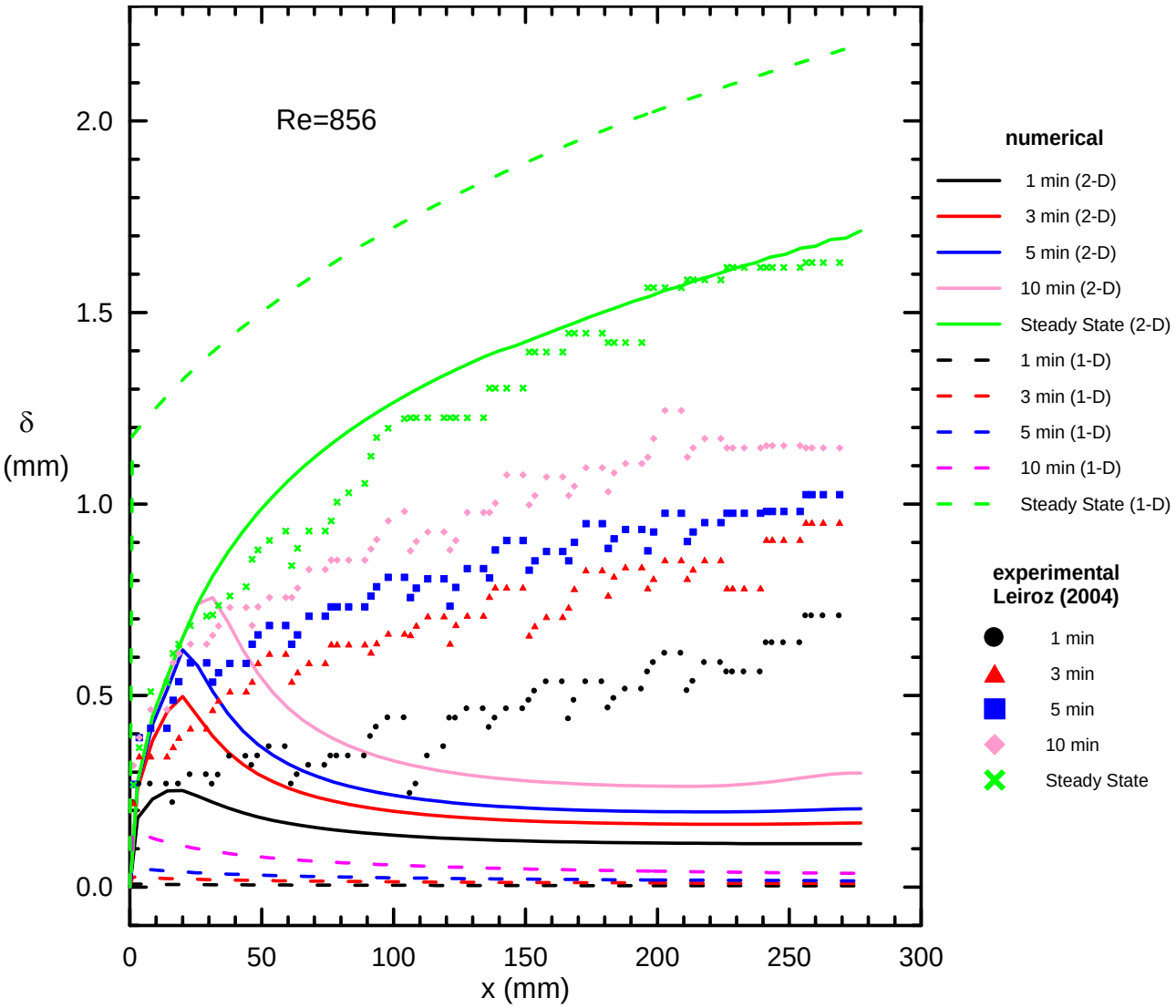

Figure 5. Measured and predicted spatial and temporal evolution of deposited wax layer for channel flow for **Re** = 856..

4. Final Remarks

The present paper presents results of an ongoing research program aimed at studying the mechanisms responsible for wax deposition in petroleum pipelines. The strategy employed in the study was to conduct laboratory experiments in simple geometries with well-defined boundary and initial conditions employing fluids with known thermo-physical properties. In parallel with the experiments, numerical models of the deposition process were developed incorporating molecular diffusion as the only deposition mechanism. A comparison of the experimentally and numerically predicted results may help assess the validity of each deposition mechanism.

The diffusion-based models developed to simulate wax deposition under laminar flow displayed a poor prediction capability. Deposition thickness did not present even the correct trends, with the exception of the steady state configuration. It is believed that the strategy adopted in the present research may contribute to a better understanding of the relative importance of the wax deposition mechanisms.

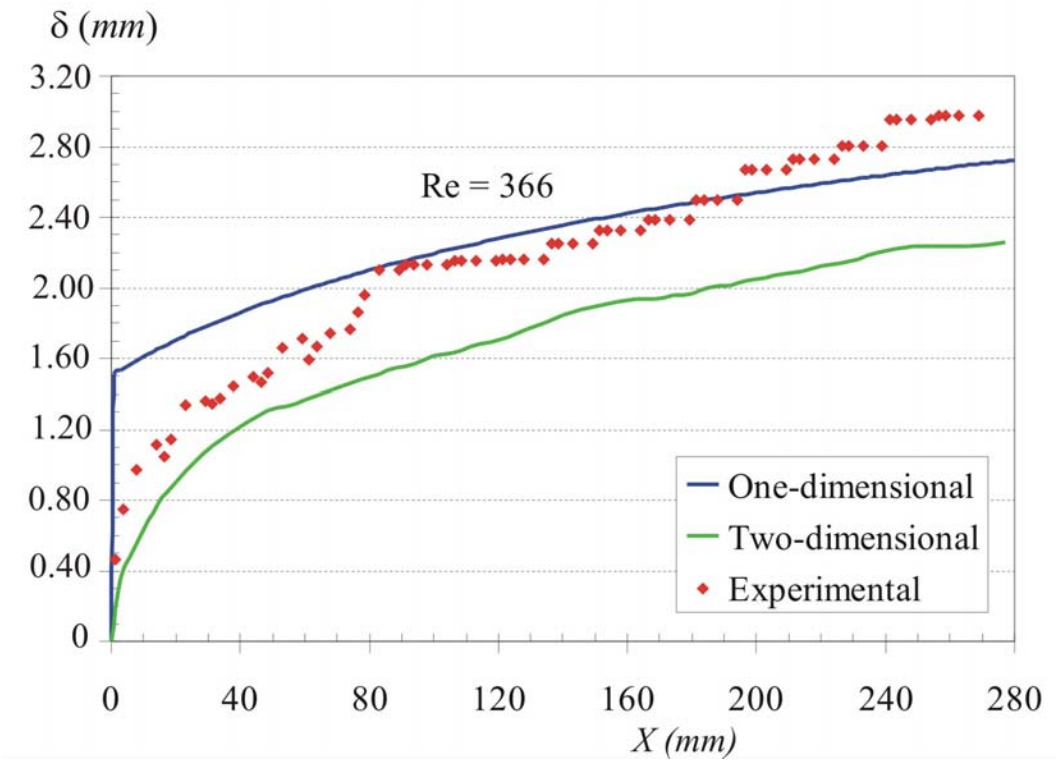

Figure 6. Comparison of the 1-D and 2-D model predictions with experimental data for the spatial evolution of the deposited wax layer for channel flow at steady state. Re = 366

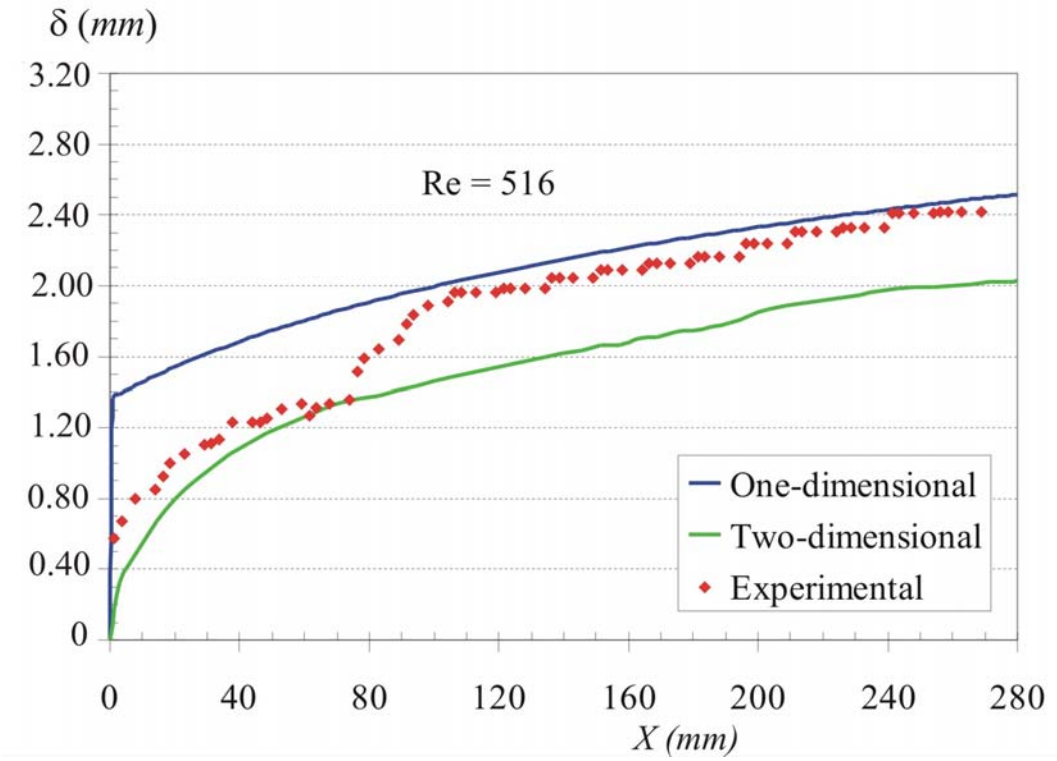

Figure 7. Comparison of the 1-D and 2-D model predictions with experimental data for the spatial evolution of deposited wax layer for channel flow at steady state. Re = 516.

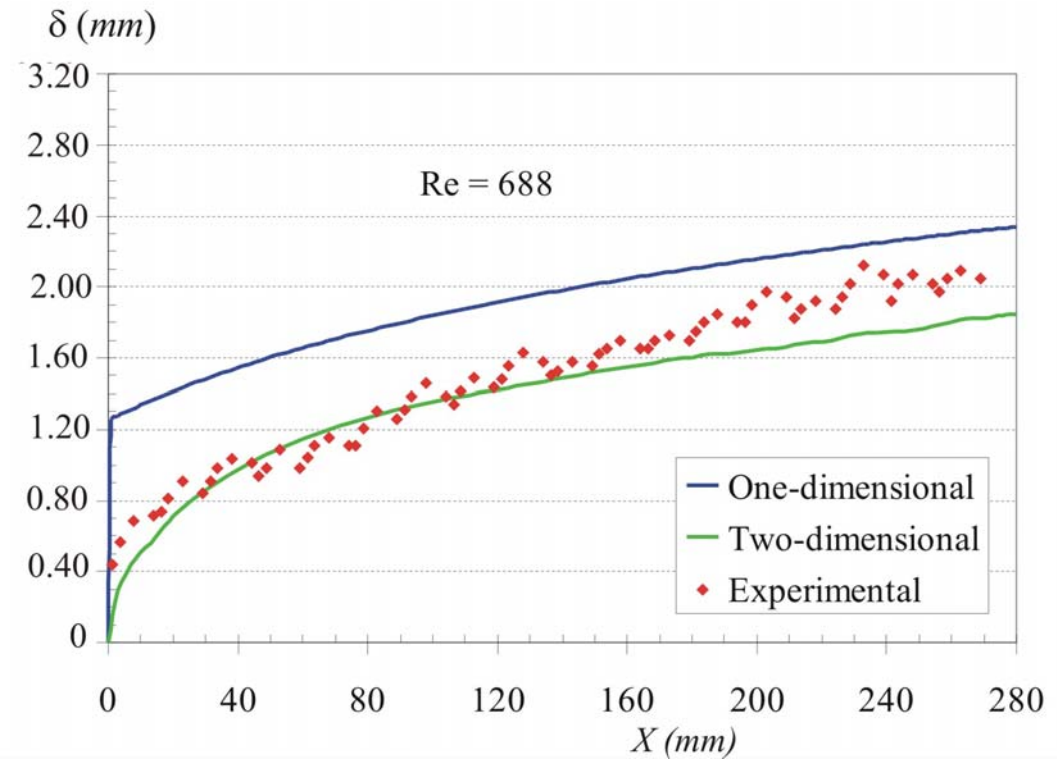

Figure 8. Comparison of the 1-D and 2-D model predictions with experimental data for the spatial evolution of deposited wax layer for channel flow at steady state. Re = 688

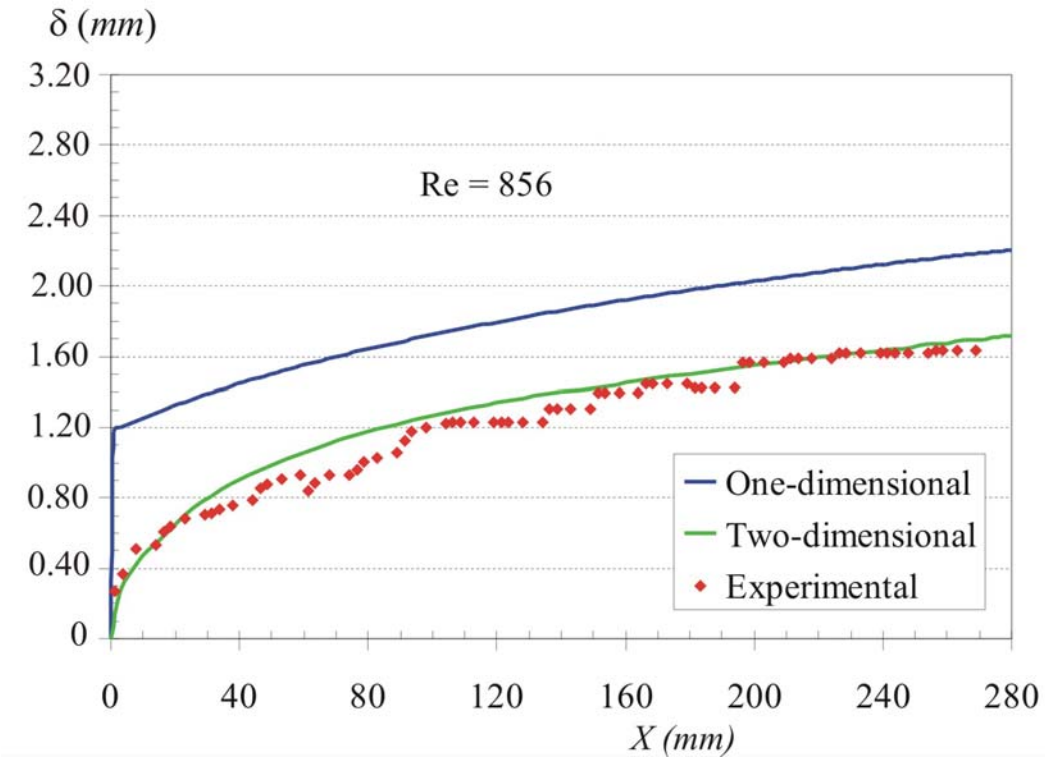

Figure 9. Comparison of the 1-D and 2-D models predictions with experimental data for the spatial evolution of deposited wax layer for channel flow at steady state. Re= 856

5. Acknowledgement

The authors acknowledge the support awarded to this research by the Brazilian Research Council, CNPq, and Petrobras.

6. References

Azevedo, L.F.A. and Teixeira, A.M., 2003, A Critical Review of the Modeling of Wax Deposition Mechanisms, Petroleum Science and Technology, 21, No.3 and 4, 393-408.

Brown, T.S., Niesen, V.G., and Erickson, D.D., 1993, Measurement and Prediction of the Kinetics of Paraffin Deposition, 68th Annual Conference of the Society of Petroleum Engineers, paper no. SPE 26548.

Burger, E.D., Perkins, T.K., and Striegler, J.H., 1981, Studies of Wax Deposition in the Trans Alaska Pipeline, Journal of Petroleum Technology, June, 1075-1086.

Creek, J.L., Lund, H.J., Brill, J.P., and Volk, M., 1999, Wax Deposition in Single Phase Flow, Fluid Phase Equilibria, 158-160, 801-811.

Fusi, L., 2003, On the Stationary Flow of a Waxy Crude Oil With Deposition Mechanisms, Nonlinear Analysis, 53, 507-526.

Incropera, P. and DeWitt, P., 1990, Introduction to Heat Transfer, JohnWiley and Sons, New York.

Leiroz, A.T., 2004, Study of Wax Deposition in Petroleum Pipelines, Ph.D. thesis, Pontifícia Universidade Católica do Rio de Janeiro – PUC-Rio, Rio de Janeiro, Brazil (in portuguese).

Leiroz, A. T., Romero, M. I., Nieckele, A.O., Azevedo, L.F.A., 2005, Wax Deposition in Laminar Channel Flow, Proceedings of 18th International Congress of Mechanical Engineering, ABCM, November 6-11, 2005, Ouro Preto, MG, Brazil

Patankar,S.V., 1980, Numerical Heat Transfer and Fluid Flow, McGraw Hill, New York.

Romero, M. I, 2005, Assessment of Molecular Difusion as a Mechanism for Wax Deposition in Petroleum Pipelines, MSc. Dissertation, Pontifícia Universidade Católica do Rio de Janeiro – PUC-Rio, Rio de Janeiro, Brazil (in portuguese).

Ribeiro, F.S., Souza Mendes, P.R., and Braga, S.L., 1997, Obstruction of Pipelines due to Paraffin Deposition during the Flow of Crude Oils, Int. J. Heat Mass Transfer, 40, 4319-4328.

Svendsen, J.A., 1993, Mathematical Modeling of Wax Deposition in Oil Pipeline Systems, AIChE Journal, 39, No.8, 1377-1388.

7. Copyright Notice